

Anisotropic and incommensurate spin fluctuations in hcp iron and some other nearly magnetic metals.

V.Thakor[†], J.B.Staunton[†], J.Poulter[‡], S.Ostanin[†], B.Ginatempo[¶], and Ezio Bruno[¶]

[†] *Department of Physics, University of Warwick, Coventry CV4 7AL, U.K.*

[‡] *Department of Mathematics, Faculty of Science, Mahidol University, Bangkok 10400, Thailand.*

[¶] *Dipartimento di Fisica and Unita INFM, Universita di Messina, Italy*

(October 29, 2018)

Abstract

We present an *ab initio* theoretical formalism for the static paramagnetic spin susceptibility of metals at finite temperatures. Since relativistic effects, e.g. spin-orbit coupling, are included we can identify the anisotropy or *easy axes* of the spin fluctuations. Our calculations find hcp-iron to be unstable to in ab-plane, incommensurate anti-ferromagnetic (AFM) modes (linked to nested Fermi surface) below $T_N = 69\text{K}$ for the lowest pressures under which it is stable. T_N swiftly drops to zero as the pressure is increased. The calculated susceptibility of yttrium is consistent with the helical, incommensurate AFM order found in many rare-earth-dilute yttrium alloys. Lastly, in line with experimental data, we find the easy axes of the incommensurate AFM and ferromagnetic spin fluctuations of the normal state of the triplet superconductor Sr_2RuO_4 to be perpendicular and parallel with the crystal c-axis respectively.

75.50Bb,75.40Cx,71.15Rf,74.70-b,75.25+2

At low temperatures under sufficient pressure iron swaps its body-centered cubic crystal structure in favor of a hexagonal close packed arrangement with the loss of its ferromagnetic long range order. It also becomes superconducting [1] in a narrow range of pressures between 15 to 30 GPa. This recent observation of superconductivity has added the phase of a common element to the growing list of magnetic or nearly magnetic materials exhibiting a superconductivity in which magnetic fluctuations seem to play a key role [2]. Prior to this finding the main interest in the magnetic properties of the high pressure hexagonal phase of iron was motivated by their effect upon its structural and mechanical properties. As part of the study of the phase diagram of iron this has a wide spread relevance for subjects as disparate as, for example, the properties of steel and the structure of the Earth's inner core [3].

The importance of magnetism upon the phase diagram is well-known. Ab-initio density functional theory (DFT) calculations have demonstrated that the formation of magnetic moments stabilises the b.c.c. phase of iron at low temperatures and normal pressures. Although stable only above the Curie temperature, face-centered cubic iron has been found to have an incommensurate spin density wave (SDW) magnetic state at low temperature following measurements on fcc-Fe precipitates on copper [4] and ab-initio calculations [5] which also show the magnetic interactions to vary sharply as a function of volume.

The magnetic attributes of hexagonal iron have not been so well identified. To date DFT calculations of the energies of two possible anti-ferromagnetic (AFM) ground states are lower than the non-magnetic one for pressures up to 60 GPa and calculated elastic constants for such magnetic states provide a better interpretation of experimental data than those from non-magnetic states [6]. On the other hand, in-situ Mossbauer data from hcp iron [7] show no evidence of long range magnetism although they do allow for it to possess strongly enhanced paramagnetism which diminishes with increasing pressure. In this letter we study the spin fluctuations (SF) in this material via calculations of the paramagnetic spin susceptibility as a function of both temperature and pressure. We find the predominant modes to be incommensurate with the hexagonal lattice and set by nesting features of the Fermi surface. We find their 'easy axis' to be in the ab-plane. These fluctuations become unstable at low temperatures and at the lower pressures where hcp-Fe is just stable, indicating an incommensurate SDW magnetic ground state.

To carry out this study we describe a theoretical formalism to calculate a relativistic paramagnetic static spin susceptibility for metals at finite temperature. We highlight how the natural inclusion of spin-orbit coupling allows us to study the anisotropy of enhanced spin fluctuations in nearly magnetic systems and to identify their *easy-axes*. The paramagnetic susceptibility of a metal can possess much structure in wave-vector (\mathbf{q}) space. Indeed a peak at one temperature can evolve into a divergence at a lower one to signify the system's transition into a magnetically ordered state characterised by a static magnetisation wave with a wave-vector corresponding to that of the peak. By seeking out the peaks of the paramagnetic susceptibility by examining a wide range of wave-vectors we can identify the dominant spin fluctuations and probe for many different possible magnetic ground states. Moreover the easy axis of the enhanced spin fluctuations in the paramagnetic phase will indicate the direction along which magnetisation grows in the ordered phase.

Following the application to hcp-Fe, we calculate the \mathbf{q} -dependence and easy axis of spin-fluctuations in hcp metals yttrium and scandium. Our results are consistent with the helical anti-ferromagnetic structure that occurs when Y is doped with magnetic rare earth impurities such as Gd. Finally we investigate the anisotropy of the spin fluctuations in the normal state of the perovskite spin-triplet superconductor Sr_2RuO_4 . This aspect has been proposed as an ingredient for the theoretical understanding of the pairing mechanism in this extensively studied material [8].

Our principal findings are in good agreement with NMR data [9].

We access the paramagnetic spin susceptibility by considering a paramagnetic metal subjected to a small, external, inhomogeneous magnetic field, $\delta\mathbf{b}^{ext}(\mathbf{r})$, which induces a magnetisation $\delta\mathbf{m}(\mathbf{r})$. We use DFT to derive an expression via a variational linear response approach [10,11]. Although there are a number of studies of this type [12], relativistic effects are typically omitted. We address this issue in this letter. Recently we have developed [13] a scheme for calculating the wave-vector, frequency and temperature-dependent dynamic spin susceptibility and have applied it to Pd, Cr and Cr-alloys obtaining good agreement with experimental data. Here we describe the new aspects that emerge when relativistic effects are incorporated in its static limit.

We start with the relativistic version of density functional theory [14] where a Gordon decomposition is applied to the current density and the spin-only part of the current retained. The Kohn-Sham-Dirac equation involving effective one-electron fields for a paramagnetic system is solved by a one-electron Green's function $G_o(\mathbf{r}, \mathbf{r}'; \varepsilon)$. If a small external field $\delta\mathbf{b}^{ext}$ is applied along a direction $\hat{\mathbf{n}}$ with respect to the crystal axes, a small magnetisation, $\delta\mathbf{m}(\mathbf{r})$, and effective magnetic field are set up. The latter is $\delta\mathbf{b}^{eff}[\rho(\mathbf{r}), \mathbf{m}(\mathbf{r})] = \delta\mathbf{b}^{ext}(\mathbf{r}) + I_{xc}(\mathbf{r})\delta\mathbf{m}(\mathbf{r})$ where we have assumed that $\delta\mathbf{b}^{ext}$ couples only to the spin part of the current and $I_{xc}(\mathbf{r})$ is the functional derivative of the effective exchange and correlation magnetic field (within the local density approximation e.g. [15] LDA) with respect to the induced magnetisation density. The response of the system to the external magnetic field is expressed in terms of the Green's function obtained from a Dyson equation in terms of unperturbed Green's function $G_o(\mathbf{r}, \mathbf{r}'; \varepsilon)$ of the paramagnetic system and $\delta\mathbf{b}^{eff}$. For a general crystal lattice with N_s atoms located at positions \mathbf{a}_l ($l = 1, \dots, N_s$) in each unit cell, a lattice Fourier transform can be carried out and an expression for the full static spin susceptibility found.

$$\chi^{\hat{\mathbf{n}}}(\mathbf{x}_l, \mathbf{x}'_{l'}, \mathbf{q}) = \chi_o^{\hat{\mathbf{n}}}(\mathbf{x}_l, \mathbf{x}'_{l'}, \mathbf{q}) + \sum_{l''}^{N_s} \int \chi_o^{\hat{\mathbf{n}}}(\mathbf{x}_l, \mathbf{x}''_{l''}, \mathbf{q}) I_{xc}(\mathbf{x}''_{l''}) \chi^{\hat{\mathbf{n}}}(\mathbf{x}''_{l''}, \mathbf{x}'_{l'}, \mathbf{q}) d\mathbf{x}''_{l''} \quad (1)$$

with the non-interacting susceptibility of the static unperturbed system given by

$$\chi_o^{\hat{\mathbf{n}}}(\mathbf{x}_l, \mathbf{x}'_{l'}, \mathbf{q}) = -(k_B T) \text{Tr} \tilde{\beta} \tilde{\boldsymbol{\sigma}} \cdot \hat{\mathbf{n}} \sum_n \int \frac{d\mathbf{k}}{\nu_{BZ}} G_o(\mathbf{x}_l, \mathbf{x}'_{l'}, \mathbf{k}, \mu + i\omega_n) \tilde{\beta} \tilde{\boldsymbol{\sigma}} \cdot \hat{\mathbf{n}} G_o(\mathbf{x}'_{l'}, \mathbf{x}_l, \mathbf{k} + \mathbf{q}, \mu + i\omega_n) \quad (2)$$

The integral is over the Brillouin zone with wave vectors \mathbf{k} , \mathbf{q} and $\mathbf{k} + \mathbf{q}$ within the Brillouin zone of volume ν_{BZ} . The \mathbf{x}_l are measured relative to the positions of atoms centred on \mathbf{a}_l . The fermionic Matsubara frequencies ω_n are $(2n + 1)\pi k_B T$ and μ is the chemical potential. The Green's function for the unperturbed, paramagnetic system containing the band structure effects is obtained via relativistic multiple scattering (Korringa-Kohn-Rostoker, KKR) theory [16]. The susceptibility has a dependence on the direction of the magnetic field, $\hat{\mathbf{n}}$, which is lost when relativistic, spin-orbit coupling effects are omitted. If an external magnetic field is applied along the $(0, 0, 1)$ direction, i.e. the c-axis in h.c.p. and tetragonal systems, we have χ^z whereas χ^x is given for the field in the ab-plane, $\hat{\mathbf{n}} = (1, 0, 0)$. We obtain an anisotropy as the difference in the susceptibility when an external magnetic field is applied in two distinct directions with respect to the crystal axes i.e. $(\chi^x - \chi^z)$. This approach presented here is applicable to ordered compounds and elemental metals and can be modified to study disordered alloys [13].

Equation (1) is solved using a direct method of matrix inversion. The full Fourier transform is then generated $\chi^{\hat{\mathbf{n}}}(\mathbf{q}, \mathbf{q}) = (1/V) \sum_l \sum_{l'} e^{i\mathbf{q} \cdot (\mathbf{a}_l - \mathbf{a}'_{l'})} \int d\mathbf{x}_l \int d\mathbf{x}'_{l'} e^{i\mathbf{q} \cdot (\mathbf{x}_l - \mathbf{x}'_{l'})} \chi^{\hat{\mathbf{n}}}(\mathbf{x}_l, \mathbf{x}'_{l'}, \mathbf{q})$ where V is the volume of the unit cell. Some aspects of the numerical methods used to evaluate (2) and (1) can be found in [13,17] and further details are given elsewhere [18]. We have used atomic sphere approximation (ASA), effective one-electron potentials and charge densities in the calculations for hcp-Fe, Y and Sc. For Sr_2RuO_4 we have used muffin-tin (MT) ($l=0$) components of the potentials

from a full potential calculation [19]. In all cases the details of the electronic structures including the Fermi surfaces compare well with those from full potential calculations.

Figure 1 shows some results of our susceptibility calculations for hcp-Fe for four volumes in the range $(128a_0^3 < V < 143a_0^3)$ where a_0 is the Bohr radius. The largest volume we consider is $142.23 a_0^3$ which corresponds to a pressure of $P \sim 16$ GPa [20] and the smallest volume is $128.98 a_0^3$ or $P \sim 45$ GPa. For all the volumes the axial ratio of the lattice constants is taken to be $c/a = 1.6$ which is very close to the experimentally observed value over a wide pressure range [20]. Calculations of $\chi(\mathbf{q})$ were performed for many wave-vectors in the Brillouin zone in a thorough search for dominant spin fluctuations and potential magnetically ordered states. The important ones are shown in Fig.1. The temperature range for such calculations was $50\text{K} \leq T \leq 300\text{K}$. According to the full potential DFT calculations of Steinle-Neumann *et al* [6], two AFM configurations (termed AFM-I and AFM-II) are more stable than non-magnetic or FM configurations for pressures up to ~ 60 GPa at $T = 0\text{K}$. AFM-I has magnetisation alternating in orientation in ab-planes stacked along the c-axis while AFM-II has magnetisation with opposite orientation on each layer aligned with the c-axis and perpendicular to the x-axis. If AFM-I were the ground state magnetic configuration then for temperatures above the Néel temperature, T_N we should see a peak in the susceptibility at the special point wave-vector $\mathbf{q}_A = (0, 0, a/2c)$, (in units of $2\pi/a$). Similarly if AFM-II was the ground state configuration then we expect to see the peak in $\chi(\mathbf{q})$ at the special point $\mathbf{q}_M = (1/\sqrt{3}, 0, 0)$. For all four volumes, however, we find the maximal peak in $\chi(\mathbf{q})$ to be at an *incommensurate* wave-vector lying in the basal plane of $\mathbf{q}_{inc.} = (0.56, 0.22, 0)$. We can trace this wave-vector $\mathbf{q}_{inc.}$ to a nesting of the metal's Fermi surface as shown in Fig.2. This is a cross-section of the Fermi surface which is generated from 4 bands straddling the Fermi energy and is comprised of four sheets. A cross-section through the basal plane reveals the Fermi surface to be dominated by two hexagonal-like shapes centred on Γ . The incommensurate $\mathbf{q}_{inc.} = (0.56, 0.22, 0)$ nests two pieces of Fermi surface as shown in Fig.2 which is a cross-section where the x-axis is along the direction of $\mathbf{q}_{inc.}$ and the y-axis is along the c-axis.

These results suggest that for the larger volumes the ground state of hcp-Fe is an incommensurate AFM. As the pressure is increased the Néel temperature decreases to zero. Figure 1 shows that at 100K enhanced AFM-SF exist which decrease in strength as volume decreases with increasing pressure. Further calculations of the full spin susceptibility, eq.(1), reveal that an instability arises at the nesting vector $\mathbf{q}_{inc.}$ above 50K at $T_N = 69\text{K}$ for the volume $V = 142.23 (a_0^3)$ ($P \sim 16$ GPa) where hcp-Fe is stable. T_N drops below 50K (the lowest temperature we can consider) for the other smaller volumes. We therefore infer that hcp-Fe has an incommensurate SDW ground state in a small pressure range starting at the onset of the hcp-phase ~ 15 GPa. Our calculations of the anisotropy reveal $\chi_o^x(\mathbf{q}_{inc.}) > \chi_o^z(\mathbf{q}_{inc.})$ for all 4 volumes and all temperatures in the range $(50\text{K} \leq T \leq 300\text{K})$. Thus hcp-Fe exhibits incommensurate AFM-SF in the ab-plane. If the superconductivity of hcp-Fe is unconventional as has been suggested [2] then the in-plane incommensurate AFM-SF must play an important role in the pairing mechanism.

Fig.1 also shows how $\chi^{-1}(\mathbf{q})$ varies with volume for other salient wave-vectors at $T = 100\text{K}$. We see that $\chi(\mathbf{q}_{inc.}) > \chi(\mathbf{q}_K) > \chi(\mathbf{q}_M) > \chi(\mathbf{q}_A) > \chi(\mathbf{q}_o \simeq (0, 0, 0))$ for all 4 volumes. Apparently hcp-Fe is furthest away from forming a ferromagnetically ordered state as shown by the relatively high value of $\chi^{-1}(\mathbf{q}_o)$. This is followed by AFM-I (\mathbf{q}_A) and then AFM-II (\mathbf{q}_M). In agreement with [6] we find that the AFM-II is a more stable configuration than AFM-I but we find a third special-point antiferromagnetic structure, AFM-III, characterised by $\mathbf{q}_K = (1/\sqrt{3}, 1/3, 0)$, to be more stable than either of these. This structure would have the magnetisation direction alternating in layers stacked along \mathbf{q}_K . Although \mathbf{q}_K signifies a more stable AFM configuration than either AFM-I and AFM-II, it is at the incommensurate vector ($\mathbf{q}_{inc.}$) where we see the maximal peak in $\chi(\mathbf{q})$ which leads to our prediction that hcp-Fe has an incommensurate SDW ground state.

Having established a way of determining the easy axis for spin fluctuations with our relativistic formalism, we can use it to deduce how magnetic impurities are likely to orientate in paramagnetic host metals. Excellent case studies are provided by yttrium alloys with low concentrations of rare earths. When crystal field effects of the rare earths do not dominate, the enhanced susceptibility of Y determines the magnetic ordering. Here we describe our calculations of this for Y and also its lighter 3d counterpart Sc. Both metals have hcp crystal structures with very similar electronic band structures and Fermi surfaces. We have used experimental lattice constants $a = 6.89$, $c = 10.83$ for Y and $a = 6.24$, $c = 9.91$ for Sc, in atomic units, a_0 . Our calculations of the static spin susceptibility defined by (1) show a peak at the wave-vector $\mathbf{q}_{inc.} = (0, 0, 0.18)2\pi/a = (0, 0, 0.57\pi/c)$ for both Y and Sc. This vector $\mathbf{q}_{inc.}$ once again corresponds to a nesting effect from a webbing feature of flat parallel sheets [21] as confirmed by Fermi surface calculations and is in good agreement with experiments [21,22]. Fig.3 shows the temperature dependence of the anisotropy of Y and Sc at the nesting vector $\mathbf{q}_{inc.}$ and also at a small vector $\mathbf{q}_o \simeq (0, 0, 0)$ (indicating ferromagnetic spin fluctuations (FM-SF)). Evidently the anisotropy is an order of magnitude larger in Y than in Sc - e.g. at $T = 50$ K the anisotropy $(\chi_o^x(\mathbf{q}_{inc.}) - \chi_o^z(\mathbf{q}_{inc.}))$ for Y is 0.0411 ($\mu_B^2/Ry.$) while for Sc it is 0.00635 ($\mu_B^2/Ry.$). This difference is caused by the spin-orbit coupling being more pronounced in the heavier 4d metal Y than in the 3d Sc. At $\mathbf{q}_{inc.}$, the AFM-SF have an easy direction in the ab-plane, $\chi_o^x(\mathbf{q}_{inc.}) > \chi_o^z(\mathbf{q}_{inc.})$, whereas that of the FM-SF is along the c-axis, $\chi_o^z > \chi_o^x$. The anisotropy is also larger at $\mathbf{q}_{inc.}$ than for small wave-vectors. These calculations show that both Y and Sc exhibit AFM-SF characterised by the incommensurate wave-vector $\mathbf{q}_{inc.} = (0, 0, 0.57\pi/c)$ and are aligned in the basal plane. They explain why when Y is perturbed by the addition of rare earth magnetic impurities (e.g. Gd), it typically responds by ordering the impurity moments into a helical AFM state in which the moments align in the basal plane and rotate their orientations in successive planes around the c-axis [23].

We conclude with our study of the anisotropy of the spin-fluctuations of the normal state of Sr_2RuO_4 . We have used lattice constants of $a = 7.30$, $c = 24.06$ in a_0 for the tetragonal unit cell. Our calculations of the susceptibility and Fermi surface for Sr_2RuO_4 show an incommensurate nesting vector of $\mathbf{q}_{inc.} = (0.35, 0.35, 0)$ similar to that found in previous calculations [24] and experiment [25]. We have compared the anisotropy at the incommensurate wave-vector $\mathbf{q}_{inc.}$ with that at small wave-vectors describing ferromagnetic SF. For the former we find $(\chi_o^z(\mathbf{q}_{inc.}) > \chi_o^x(\mathbf{q}_{inc.}))$ implying that the incommensurate AFM-SF should have an easy direction along the c-axis. Conversely for small \mathbf{q} we find $(\chi_o^x > \chi_o^z)$ and therefore the FM-SF to be *in the ab-plane*. These findings are in good agreement with NMR experiments [9]. At $T = 50$ K, the anisotropy $(\chi_o^z(\mathbf{q}_{inc.}) - \chi_o^x(\mathbf{q}_{inc.}))$ is 0.847 ($\mu_B^2/Ry.$) which is an order of magnitude greater than what we find for Y owing to the large tetragonal distortion ($c/a = 3.3$) of the unit cell. Finally a calculation of $(\chi_o^x(\mathbf{q}_{inc.})/\chi_o^z(\mathbf{q}_{inc.}))$ at $T=50\text{K}$ yields 0.98. According to a scenario based on a simple model by Kuwabara *et al* [8], the spin-triplet superconducting state of Sr_2RuO_4 can be stabilised by incommensurate AFM-SF with the easy axis for the fluctuations along the c-axis. Our value of the anisotropy of the SF, $(\chi_o^x(\mathbf{q}_{inc.})/\chi_o^z(\mathbf{q}_{inc.}))$, of 0.98, however, would also imply that the system must be very close to ordering magnetically.

We acknowledge support from the EPSRC (UK).

REFERENCES

- [1] K.Shimizu et al., *Nature*, **412**, 316, (2001).
- [2] I.I.Mazin et al., *Phys.Rev.B* **65**, 100511, (2002); S.K.Bose et al. *cond-mat/0207318*; T.Jarlborg *cond-mat/0112387*.
- [3] S.Gilder and J.Glen, *Science* **279**, 72, (1998).
- [4] Y.Tsunoda et al., *J.Mag.Magn.Mat.* **128**,133, (1993).
- [5] M.Uhl et al., *Phys.Rev.B* **50**, 291, (1994); C.S.Wang et al. *Phys.Rev.Lett.* **54**, 1852 (1985); F.J.Pinski et al, *Phys.Rev.Lett.* **56**, 2096, (1986).
- [6] G.Steinle-Neumann et al., *Phys.Rev.B* **60**, 791, (1999).
- [7] G.Cort et al., *J.Appl.Phys.* **53**, 2064, (1982); R.D.Taylor et al., *J.Appl.Phys.* **53**, 8199, (1982).
- [8] T.Kuwabara and M.Ogata, *Phys.Rev.Lett.* **85**, 4586, (2000).
- [9] H.Mukuda et al., *J.Phys.Soc.Jpn.* **67**, 3945, (1998).
- [10] S.H Vosko, J.P Perdew, *Can.J.Phys.* **53**, 1385, 1975.
- [11] A.H.MacDonald, S.H.Vosko, *J. Low Temp.Phys.* **25**, 27, 1976; A.H.MacDonald et al., *Solid State Commun.* **18**, 85, 1976; M.Matsumoto et al., *J.Phys.: Cond.Mat.* **2**, 8365, 1990.
- [12] E.Stenzel et al., *J.Phys.F* **16**,1789, (1986); S.Y.Savrasov, *Phys.Rev.Lett.* **81**, 2570, (1998).
- [13] J.B.Staunton et al., *Phys.Rev.Lett.* **82**, 3340, (1999); J.B.Staunton et al., *Phys.Rev.B*, **62**, 1075, (2000).
- [14] A.K.Rajagopal and J.Callaway, *Phys.Rev.B*, **7**, 1912, (1973); A.H.Macdonald, S.H.Vosko , *J.Phys.C: Solid State Phys.* **12**, 2977, (1979).
- [15] U.von Barth and L.Hedin, *J.Phys.C* **5**, 1629, (1972).
- [16] J.S. Faulkner and G.M. Stocks, *Phys.Rev.B* **21**, 3222, (1980); P.Strange et al., *J.Phys.:Condens.Mat* **1**, 2959, 1989.
- [17] E.Bruno and B.Ginatempo, *Phys.Rev.B* **55**, 12946, (1997).
- [18] V.Thakor et al. (2002), in preparation.
- [19] e.g. P. Blaha, K. Schwarz, P. Sorantin and S.B. Trickley, *Comput. Phys. Comm.* **59**, 399 (1996).
- [20] W.A.Basset and E.Huang, *Science*, **238**, 780, (1987).
- [21] S.B.Dugdale et al., *Phys.Rev.Lett.* **9**, 941, (1997).
- [22] L.I.Vinokurova et al., *JETP Lett.*, **34**, 566, (1981).
- [23] H.M.Fretwell et al., *Phys.Rev.Lett.* **82**, 19, (1999).
- [24] I.I.Mazin et al., *Phys.Rev.Lett.* **82**, 4324, (1999).
- [25] Y.Sidis et al, *Phys.Rev.Lett.* **83**, 3320, (1999)

FIGURES

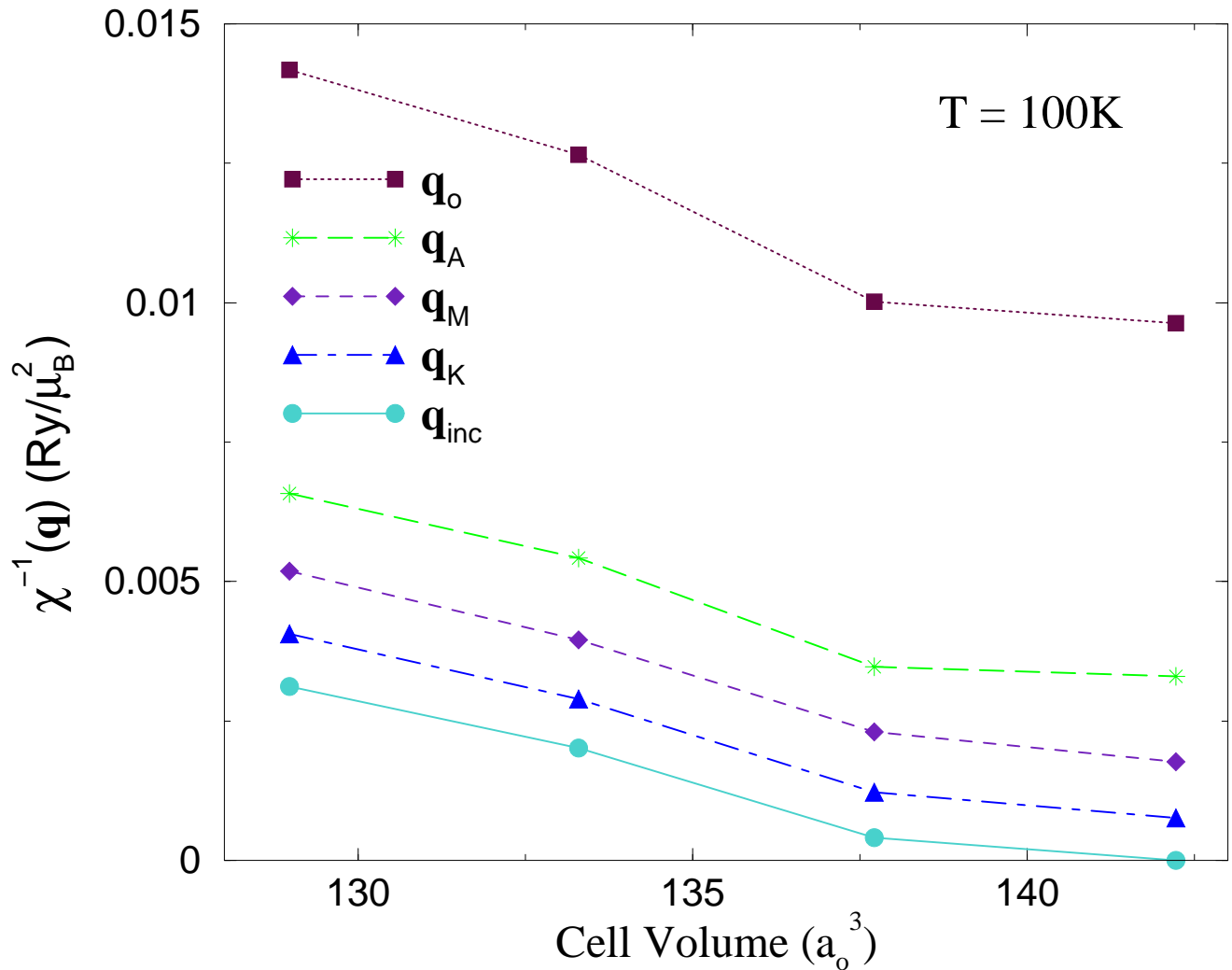


FIG. 1. The inverse susceptibility of hcp-Fe at $T = 100\text{K}$ for various wave-vectors ($\mathbf{q}_o \simeq 0$, the nesting vector $\mathbf{q}_{inc.} = 2\pi/a(0.56, 0.22, 0)$ and at the special points A, M and K) for a number of unit cell volumes.

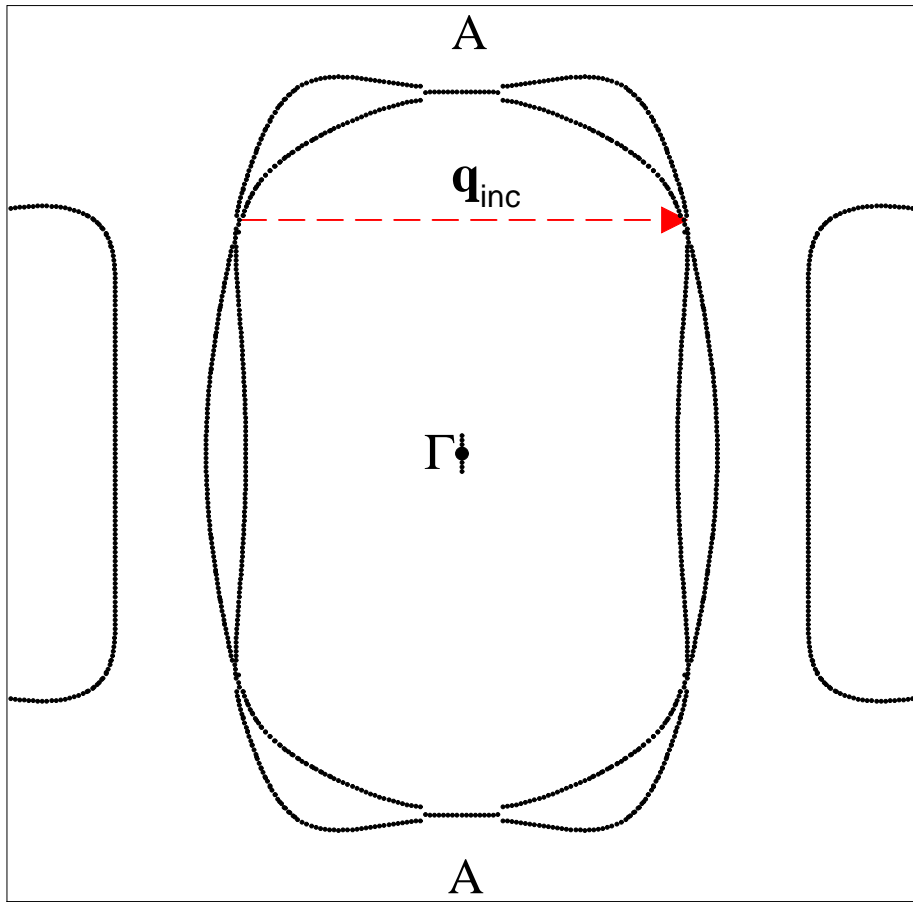


FIG. 2. Cross-section of the Fermi surface of hcp-Fe at $V=137.72 a_0^3$ where the x- and y-axes are along $\mathbf{q}_{inc.} = 2\pi/a(0.56, 0.22, 0)$ and the c-axis $(0, 0, 1)$ respectively.

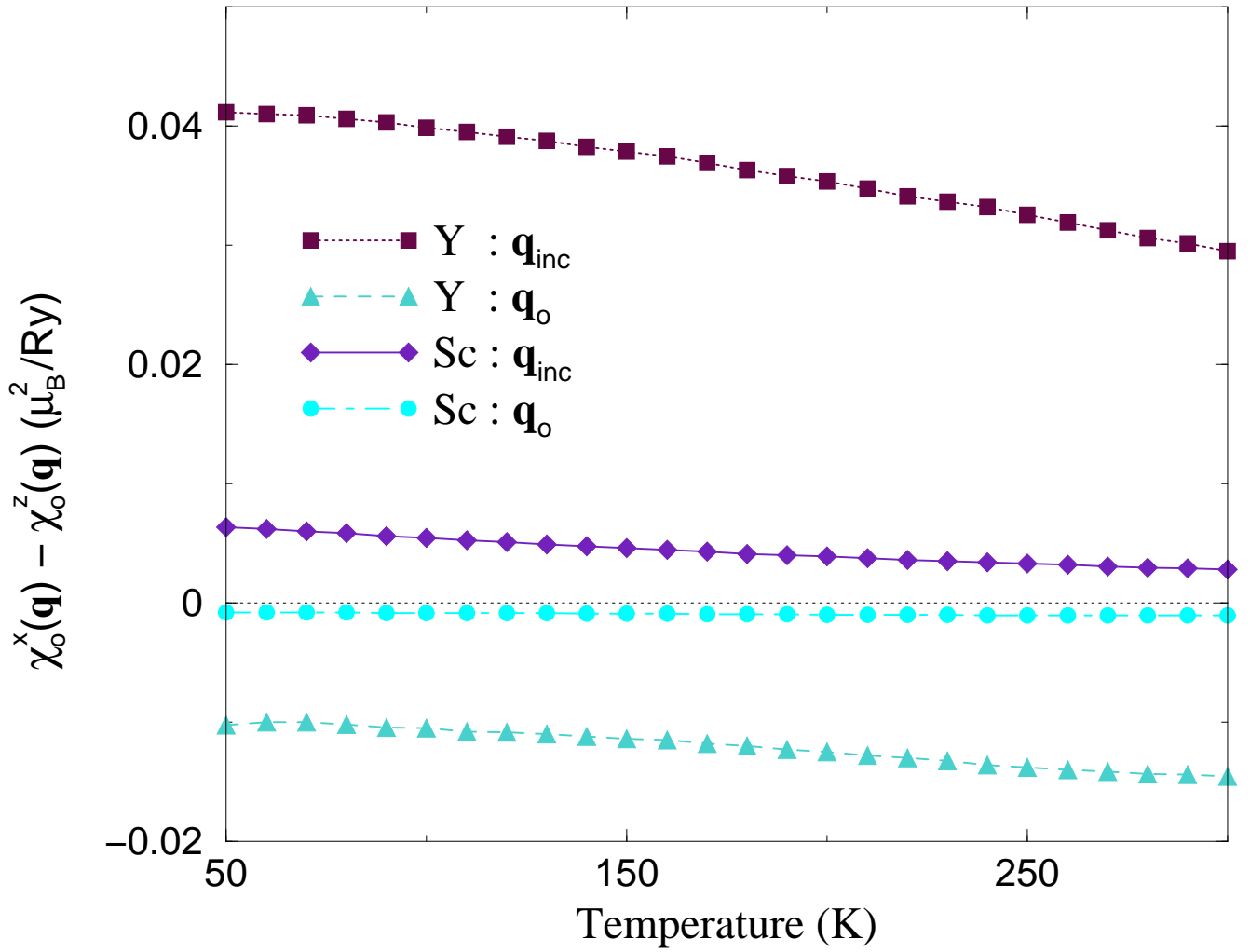


FIG. 3. The temperature dependence of the anisotropy $\chi_o^x(\mathbf{q}) - \chi_o^z(\mathbf{q})$ of Y and Sc at both the nesting vector $\mathbf{q}_{inc.} = (0, 0, 0.57\pi/c)$ and $\mathbf{q}_o \simeq (0, 0, 0)$.